Nonlinear Channel Estimation Issues in Cooperative Sensor MIMO

Ronald A. Iltis
Department of Electrical and Computer Eng.
University of California
Santa Barbara, CA 93106-9560, USA
Email: iltis@ece.ucsb.edu

Richard Cagley
Toyon Research Corporation
6800 Cortona Dr.
Goleta, CA 93117
Email: rcagley@toyon.com

***Abstract*— A cooperative MIMO system for range extension in sensor networks is considered. A local sensor group forms a consensus and seeks to transmit a common pool of data to a stand-off multi-element collector. Each sensor then transmits one column of an orthogonal space-time block code (OSTBC). The resulting increased effective power and diversity can yield substantial range increases for moderate numbers of sensors. The major problem is tracking the individual sensor frequency offsets, delays and sensor-to-collector channels under high mobility. The unscented Kalman filter (UKF) is presented as a state of the art solution to the cooperative MIMO channel estimation problem, and its performance is evaluated via a hybrid analysis/simulation of bit-error rate. A hardware implementation of the collector is also discussed based on simplified correlation and homodyne estimation strategies. The homodyne estimator performance is finally compared to that of previous generalized successive interference cancellation (GSIC) and correlation-based algorithms via simulation.**

I. Introduction

The use of multiple single-antenna sensors to form a virtual transmit antenna array has been proposed in [1][2] and [3]. Typically, each sensor transmits one column of an OSTBC [4], and the resulting spatial/temporal diversity allows trade-offs between reduced sensor power, error rates and range. Here, it is assumed that a local sensor group has formed a consensus (e.g. acoustic localization of a target) and thus has a common pool of data to transmit to the collector (e.g. target position/velocity/ID.) It is assumed that each sensor has fixed transmit power. The objective is to increase collector operating range for constant BER by increasing the number of cooperating sensors.

The primary difficulty in the proposed cooperative MIMO system is estimation of channel states. Unlike point-to-point MIMO links, the individual sensor oscillators cannot be coupled, and thus frequency/phase offsets are independent and must be tracked individually. In addition, the collector experiences different transmission delays from each sensor and thus individual symbol timing, as well as channel gains must be estimated. Previous estimators for offset/delay/channels in MIMO systems typically assume that these parameters are quasi-static, and thus maximum-likelihood (correlation) techniques are applicable [5][6][7][8]. However, the collector is often highly mobile and thus time-varying channel models are more realistic.

This paper considers two types of channel estimators. First, the unscented Kalman filter (UKF) [9] is proposed for joint estimation of offset/delay/channels. The UKF is challenging from the standpoint of actual hardware implementation, but results here show that its performance is within a half dB of that achieved with perfect channel state information (CSI.) Second, we describe the current status of a hardware testbed for cooperative MIMO. Although implementation of the UKF is not yet feasible, quasi ML techniques using a homodyne frequency offset estimator have been demonstrated. It is shown that the homodyne method can be obtained via a systematic approximation to the ML offset estimator.

The paper is organized as follows. Section II presents the signal/channel model incorporating realistic pulse shaping, and derives the link budget for computing collector range under Rayleigh fading. Section III discusses the UKF channel estimator and the hybrid analysis/simulation BER evaluation. The current hardware testbed channel estimator, derivation and performance evaluation of the homodyne method are summarized in Section IV. Conclusions are given in Section V.

II. Signal/Channel Models and Link Budget

It is assumed that each of N_s single-element sensors transmits one column of an OSTBC to an M_c element collector. The collector oversamples at N_d times the symbol rate, and thus for each N_c symbol-long OSTBC codeword forms a received matrix $\mathbf{R}(n) \in \mathbb{C}^{N_c N_d \times N_s}$. The resulting received signal for OSTBC codeword n is derived in [8] as

$$\mathbf{R}(n) = \sum_{k=1}^{N_s} \sum_{q=0}^{N_c-1} \mathbf{p}_{q,n}(\tau_k, \delta\omega_k)\mathbf{h}_k^T s_k(q+nN_c) + \mathbf{N}(n). \quad (1)$$

The noise $\mathbf{N}(m)$ has i.i.d. circular Gaussian elements with variance $2N_0/T_s$ for an input Nyquist bandwidth $1/(2T_s)$. The oversampled raised-cosine pulse corresponding to symbol $s_k(q+mN_c)$ is $\mathbf{p}_{q,n}(\tau_k, \delta\omega_k)$ and is parameterized by the delay τ_k and frequency offset $\delta\omega_k$. Specifically [8],

$$\mathbf{p}_{q,n}(\tau_k, \delta\omega_k) = \quad (2)$$
$$\Big[p((N_cN_d-1)T_s - \tau_k - qT)e^{i\delta\omega_k(nN_cT+(N_cN_d-1)T_s)},$$
$$\ldots, p(-\tau_k - qT)e^{i\delta\omega_k nN_cT}\Big]^T,$$

where $p(t)$ is the continuous-time pulse, T is the OSTBC symbol interval, and $N_d = T/T_s$ is the oversampling factor. The bandpass energy in each pulse $p(t)$ is defined by $E_s = N_u \int p(t)^2 dt/2$, where $N_u = 1$ for the Alamouti code and $N_u = 2$ for $\mathcal{G}_c^4$. Thus, each sensor transmits with fixed power regardless of the number of sensors N_s, in order to maximize operating range.

To determine maximum collector range to meet a BER target, perfect CSI and orthogonal pulses $\mathbf{p}_{q,n}$ are assumed. For linear decoding [4] and QPSK symbols $s_k(q)$, it has been shown [10][2] that the resulting BER conditioned on the channel realization is

$$P_b = \frac{1}{2}\text{erfc}\left(\sqrt{\frac{E_b}{N_0}||\mathbf{H}||_F^2}\right), \tag{3}$$

where $\mathbf{H} = [\mathbf{h}_1 \dots \mathbf{h}_{N_s}]$. Note that (3) is modified slightly for constant sensor power with increasing N_s. In Rayleigh fading, the components of $\mathbf{H}$ are i.i.d. circular Gaussian. The exponential bound $\text{erfc}(\sqrt{x}) < \exp(-x)$ is then employed, which when averaged over the density of $\mathbf{H}$ yields the expression for unconditional BER

$$\overline{P}_b < \frac{1}{2}\left[1 + \frac{E_b}{N_0}\right]^{-M_c N_s}. \tag{4}$$

The asymptotic upper bound on BER in Rayleigh fading is thus $\overline{P}_b \to \frac{1}{2}\exp(-E_b M_c N_s/N_0)$. Again, since sensor power is fixed regardless of N_s, an exponential coding gain in N_s and exponential collector diversity gain in M_c are jointly obtained.

The Hata model [11] is employed to calculate the link budget between an individual sensor and individual collector element. The receive power (dB) is

$$\begin{aligned} P_R(dB) &= P_T(dB) + G_T(dB) + G_R(dB) + \\ &10\log_{10}\left(\frac{\lambda}{4\pi d_0}\right)^2 + 10\alpha\log_{10}(d_0/d_r), \end{aligned} \tag{5}$$

where P_T is transmit power, G_T is the transmit antenna gain (0 dB for a single-antenna sensor), G_R is the collector element gain and d_0 is a nominal distance at which spherical loss is valid. The actual range between the sensor and collector is d_r. The propagation loss typically satisfies $2 < \alpha < 5$ and λ is wavelength. From eq. (4), we compute the required received power P_R needed to maintain a target BER P_b^*. Let $\gamma = E_b/N_0$ be the required receive SNR per bit between a single sensor and single collector element computed from (3). Then

$$\begin{aligned} \gamma &= \left(\frac{1}{2P_b^*}\right)^{1/(N_s M_c)} - 1 \\ P_R^*(dB) &= 10\log_{10}(N_0 R_c \gamma), \end{aligned} \tag{6}$$

where R_c is the bit rate. The achievable range d_r is then obtained from (5) by substituting P_R^*.

The range as a function of number of sensors and bit rate is shown in Fig. 1 for the Hata model. A λ corresponding to a 1 GHz carrier is assumed, with $\alpha = 3$ as the fading exponent and $d_0 = 100$ m. Each sensor has fixed power of 20 dBm, and $M_c = 8$ collector elements with individual gains of $G_R = 15$ dB are assumed. It is seen that at 1 kbps, range is doubled as N_s increases from 2 to 16 sensors. At low data rates, ranges up to 4.5 km can be achieved with 16 sensors.

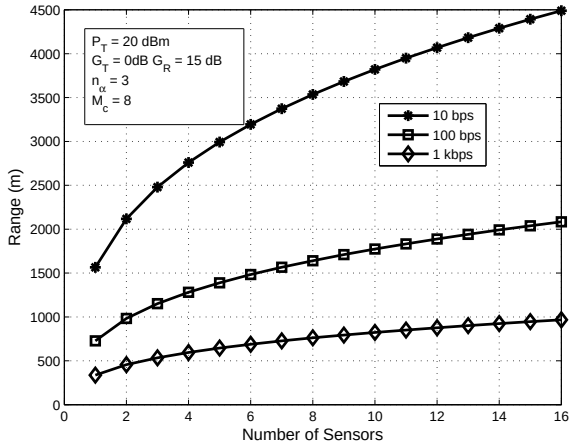

Fig. 1. Collector range for Rayleigh fading and OSTBCs.

III. Unscented Kalman Filter for Channel Estimation

Returning to the received signal model eq. (1), it is seen that $\mathbf{R}(n)$ is a nonlinear function of the delays τ_k and offsets $\delta\omega_k$. Furthermore, these quantities along with the channels $\mathbf{h}_k$ are time-varying. Due to the nonlinear measurement model, the standard Kalman filter cannot be employed. Alternative nonlinear estimators include the extended Kalman, Gaussian sum and particle filters [12]. However, we focus here on the unscented Kalman filter (UKF) [9] which has less complexity than particle filters, and generally outperforms the EKF.

To apply the UKF, it is convenient to first define a single real-valued state vector $\mathbf{x}(n)$ as follows.

$$\begin{aligned} &\mathbf{x}(n) = [\tau_1 \dots \tau_{N_s} \delta\omega_1 \dots \delta\omega_{N_s} \\ &Re\{\mathbf{h}_1\}^T \dots Re\{\mathbf{h}_{N_s}\}^T Im\{\mathbf{h}_1\}^T \dots Im\{\mathbf{h}_{N_s}\}^T]^T \end{aligned} \tag{7}$$

The dimension of $\mathbf{x}(n)$ is thus $N_x = N_s(2M_c + 2)$. Next, the complex-valued received signal $\mathbf{R}(n)$ in (1) is mapped to a real-valued vector

$$\mathbf{z}(n) = [Re\{Vec(\mathbf{R}(n)\}^T Im\{Vec(\mathbf{R}(n)\}^T]^T, \tag{8}$$

where $Vec(\mathbf{A})$ is the vector formed by stacking the columns of matrix $\mathbf{A}$. Thus $\mathbf{z}(n)$ has dimension $2N_c N_d M_c$. The nonlinear measurement $\mathbf{g}(\mathbf{x}(n))$ is then defined as

$$\begin{aligned} &\mathbf{G}(\mathbf{x}(n), s_k(q + nN_c)) = \\ &\sum_{k=1}^{N_s}\sum_{q=0}^{N_c-1} \mathbf{p}_{q,n}(\tau_k(n), \delta\omega_k(n))\mathbf{h}_k(n)^T s_k(q + nN_c) \\ &\mathbf{g}(\mathbf{x}(n), s_k(q + nN_c)) = \\ &\left[Re\{Vec(\mathbf{G}(\mathbf{x}(n), s_k(q + nN_c)))^T\}\right. \\ &\left.Im\{Vec(\mathbf{G}(\mathbf{x}(n), s_k(q + nN_c)))^T\}\right]^T, \end{aligned} \tag{9}$$

where the dependence of $\mathbf{x}(n)$ on $\mathbf{h}_k, \delta\omega_k, \tau_k$ is given by (7). Note that the measurement function (9) also depends on the STC symbols $s_k(q)$. A linear, first-order autoregressive process model is appropriate for MIMO channels and offsets governed by Jakes' model [13]. Thus, the process and measurement model for the cooperative MIMO problem are expressed as

$$\begin{aligned} \mathbf{x}(n+1) &= \mathbf{F}\mathbf{x}(n) + \mathbf{w}(n) \\ \mathbf{z}(n) &= \mathbf{g}(\mathbf{x}(n)) + \mathbf{v}(n) \end{aligned} . \tag{10}$$

A detailed derivation of the UKF is given in [9]. For the model (10), the prediction equations are identical to the ordinary Kalman filter. Let $\hat{\mathbf{x}}(n-1|n-1) \approx E\{\mathbf{x}(n-1)|\mathbf{z}^{n-1}\}$ be the measurement update, with $\mathbf{z}^n = \{\mathbf{z}(n)\ldots\mathbf{z}(1)\}$. The measurement covariance is $\mathbf{P}(n-1|n-1) \approx E\{[\mathbf{x}(n-1) - \hat{\mathbf{x}}(n-1|n-1)][]^T\}$. Then the first step in the UKF recursion after receiving $\mathbf{z}(n)$ is to compute one-step predictions

$$\begin{aligned} \hat{\mathbf{x}}(n|n-1) &= \mathbf{F}\hat{\mathbf{x}}(n-1|n-1) \\ \mathbf{P}(n|n-1) &= \mathbf{F}\mathbf{P}(n-1|n-1)\mathbf{F}^T + \mathbf{Q}, \end{aligned} \tag{11}$$

where $\mathbf{Q} = E\{\mathbf{w}(n)\mathbf{w}(n)^T\}$ is the process noise covariance.

The measurement update step must account for the non-linear measurement function $\mathbf{g}(\mathbf{x}(n))$. The extended Kalman filter accomplishes this via linearization, whereas the UKF forces a linear structure to the measurement update as follows [9].

$$\hat{\mathbf{x}}(n|n) = \hat{\mathbf{x}}(n|n-1) + \mathbf{P}_{x,\tilde{z}}(n)\mathbf{P}_{\tilde{z}}(n)^{-1}[\mathbf{z}(n) - \hat{\mathbf{z}}(n|n-1)]. \tag{12}$$

The covariance matrices $\mathbf{P}_{x,\tilde{z}}(n)$ and $\mathbf{P}_{\tilde{z}}(n)^{-1}$ are defined in terms of sigma-points [9] $\mathbf{x}_0(n) = \hat{\mathbf{x}}(n|n-1)$, and $\mathbf{x}_i(n) = \mathbf{x}_0(n) \pm \sqrt{(2N_x+1)}\mathbf{P}(n|n-1)_i^{1/2}$, for $i = 1, \ldots, 2N_x$. The weights W_i form a probability vector. The vector $\mathbf{P}(n|n-1)_i^{1/2}$ is the i-th column of the Cholesky decomposition of the predicted covariance [9]. A predicted measurement is then formed by

$$\hat{\mathbf{z}}(n|n-1) = \sum_{i=0}^{2N_x} W_i \mathbf{g}(\mathbf{x}_i(n)), \tag{13}$$

and the covariances are

$$\begin{aligned} &\mathbf{P}_{x,\tilde{z}}(n) = \\ &\sum_{i=0}^{2N_x} W_i[\mathbf{x}_i(n) - \hat{\mathbf{x}}_i(n|n-1)][\mathbf{g}(\mathbf{x}_i(n)) - \hat{\mathbf{z}}(n|n-1)]^T, \\ &\mathbf{P}_{\tilde{z}}(n) = \\ &\sum_{i=0}^{2N_x} W_i[\mathbf{g}(\mathbf{x}_i(n)) - \hat{\mathbf{z}}(n|n-1)][\mathbf{g}(\mathbf{x}_i(n)) - \hat{\mathbf{z}}(n|n-1)]^T + \\ &\frac{N_0}{T_s}\mathbf{I}. \end{aligned} \tag{14}$$

In order to implement the UKF, tentative decisions on the OSTBC symbols $s_k(q)$ are required to compute the measurement function $\mathbf{g}(\mathbf{x}(n))$. Linear decoding [4] for OSTBCs can be shown to only be optimal for orthogonal pulse vectors $\mathbf{p}_{q,n}$ in (1) and perfect synchronization among sensors $\tau_k = \tau$ for $k = 1, \ldots, N_s$. For the raised-cosine pulses used, and asynchronous sensor transmission, the ML decoder for OSTBCs has complexity $\mathcal{O}(Q^{N_s})$, where Q is the size of the signal constellation. Thus, we employ linear decoding despite its suboptimality for simplicity. The details of the linear decoder are given in [8], but the final form assuming orthogonal pulses is

$$\hat{b}_l = \arg\max_{b_l} 2Re\left\{b_l \sum_{q=0}^{N_c-1} y'_{k_q(l)}(q)\right\} - |b_l|^2 \sum_{q=0}^{N_c-1} Q_{k_q(l),k_q(l),q,q}, \tag{15}$$

where the $b_l \in \mathbb{C}$ are the information symbols corresponding to the OSTBC code symbols $s_k(q)$. The sensor index $k_q(l)$ corresponds to the sensor transmitting symbol b_l at time q in the OSTBC. In (15), the sufficient statistics are defined by

$$y'_{k_q(l)}(q) = \begin{cases} (-)y_{k_q(l)}(q) \text{ if } s_{k_q(l)}(q) = (-)b_l \\ (-)y_{k_q(l)}(q)^* \text{ if } s_{k_q(l)}(q) = (-)b_l^* \end{cases}, \tag{16}$$

where

$$\begin{aligned} \mathbf{y}_k(q) &= \hat{\mathbf{h}}_k^T \mathbf{R}(n)^H \mathbf{p}_q(\hat{\tau}_k, \hat{\delta}\omega_k) \\ Q_{k,k',q,q'} &= \mathbf{p}_{q'}(\hat{\tau}_{k'}, \hat{\delta}\omega_{k'})^H \mathbf{p}_q(\hat{\tau}_k, \hat{\delta}\omega_k)\hat{\mathbf{h}}_{k'}^H \hat{\mathbf{h}}_k. \end{aligned} \tag{17}$$

The UKF channel/offset tracking algorithm operates in decision-directed mode, where estimates $\hat{\mathbf{x}}(n|n-1)$ are used to compute the data decisions $\hat{b}_l(n)$ using the linear decoding rule (15). The decisions $\hat{b}_l(n)$ then determine the STC symbols $\hat{s}_k(q)$ in (9). The overall decoder and UKF estimation algorithm is given in Table I.

A hybrid analysis/simulation evaluation of BER is employed for the UKF in a manner similar to that used for GSIC in [8].

Given channel/offset estimates $\hat{\mathbf{x}}(n|n-1)$

$\hat{\mathbf{h}}_k, \hat{\tau}_k, \hat{\delta}\omega_k \leftarrow \hat{\mathbf{x}}(n|n-1)$

Update estimated sufficient statistics

$\hat{y}_k(q) = \hat{\mathbf{h}}_k^T \mathbf{R}(n)^H \mathbf{p}_q(\hat{\tau}_k, \hat{\delta}\omega_k)$

Compute data decisions using linear decoding (QPSK)

$\{\hat{b}_l\} = \arg\max_{\{b_l\}} \sum_{l=1}^{N_s} 2Re\left\{b_l \sum_{q=0}^{N_c-1} \hat{y}'_{k_q(l)}(q)\right\}$

Form predicted measurement using data decisions $\hat{b}_l \rightarrow \hat{s}_k(q)$

$\hat{\mathbf{z}}(n|n-1) = \sum_{i=0}^{N_s(2M_c+2)} W_i \mathbf{g}(\mathbf{x}_i(n), \hat{s}_k(q))$

Compute Cholesky decomposition of $\mathbf{P}(n|n-1)$ and sigma-points $\mathbf{x}_i(n)$

Update covariance matrices $\mathbf{P}_{x,\tilde{z}}(n), \mathbf{P}_{\tilde{z}}(n)$

Form real-valued measurement vector

$\mathbf{z}(n) = [Re\{Vec(\mathbf{R}(n)\}^T Im\{Vec(\mathbf{R}(n)\}^T]^T$

Measurement update

$\hat{\mathbf{x}}(n|n) = \hat{\mathbf{x}}(n|n-1) + \mathbf{P}_{x,\tilde{z}}(n)\mathbf{P}_{\tilde{z}}(n)^{-1}[\mathbf{z}(n) - \hat{\mathbf{z}}(n|n-1)]$

Covariance update

$\mathbf{P}(n|n) = \mathbf{P}(n|n-1) - \mathbf{P}_{x,\tilde{z}}(n)\mathbf{P}_{\tilde{z}}(n)^{-1}\mathbf{P}_{x,\tilde{z}}(n)^T$

Prediction

$\hat{\mathbf{x}}(n+1|n) = \mathbf{F}\hat{\mathbf{x}}(n|n)$

TABLE I

UKF CHANNEL TRACKER/DECODER

The BER for linear decoding was obtained in closed form in [8] conditioned on offset/delay/channel states and estimates. The result is

$$P_b = \frac{1}{2^{2N_s-1}} \sum_{\mathsf{S}^n:\mathrm{sgn}(Re\{b_1^n\})=1} \frac{1}{2}\mathrm{erfc}\left(\frac{E\{U_1^n\}}{\sqrt{2Var\{U_1\}}}\right),$$
$$E\{U_1^n\} =$$
$$2Re\left\{\sum_{q=0}^{N_c-1} \mathrm{sgn}(Re\{s_{k_q(1)}^n\})\hat{\mathbf{h}}_{k_q(1)}^T(\mathsf{S}^n)^H\mathbf{p}_q(\hat{\theta}_{k_q(1)})\right\}$$
$$Var\{U_1\} =$$
$$\frac{4N_0}{T_s}\sum_{q=0}^{N_c-1}\sum_{q'=0}^{N_c-1}\hat{\mathbf{h}}_{k_q(1)}^H\hat{\mathbf{h}}_{k_{q'}(1)}\mathbf{p}_q(\hat{\theta}_{k_q(1)})^H\mathbf{p}_{q'}(\hat{\theta}_{k_{q'}(1)}), \tag{18}$$

Note that $\hat{\theta}_k = \{\hat{\tau}_k, \hat{\delta}\omega_k\}$. The signal matrix S^n corresponds to the n-th of 4^{N_s} OSTBC codewords and is equivalent to eq. (1) with zero noise.

In the simulations, a channel trajectory and corresponding UKF estimates are generated, and BER (18) is evaluated for each OSTBC codeword interval. The time-average of BER, assuming ergodicity, then yields an estimate of unconditional error rate. Figure 2 shows the performance of the UKF, linear decoding with CSI, and linear decoding for orthogonal synchronized pulses. A 2×2 Alamouti code and 4×4 $\mathcal{G}_c^4$ code, both with $M_c = 8$ collector elements are compared. The carrier frequency was 1 GHz with a $1/T = 500$ ksps symbol rate. Frequency offsets were chosen uniformly in the range ± 10 kHz. The first-order AR channel was simulated according to an approximate Jakes' model with collector velocity of 100 m/s. It is seen that the performance loss due to offset/delay/channel estimation is less than .5 dB. The largest performance degradation occurs due to non-orthogonality of the pulses $\mathbf{p}_{q,n}$ and relative frequency offsets between sensors. Note that the UKF was initialized using the GSIC estimator of [8].

Channel errors and UKF predicted error covariances are compared in Fig. 3. Specifically, we compare the error norm $||\mathbf{H}(n) - \hat{\mathbf{H}}(n)||_F^2$ with the trace covariance tr$\{\mathbf{P}_c(n|n-1)\}$. Note that $\mathbf{P}_c$ is the $2N_sM_c \times 2N_sM_c$ submatrix of $\mathbf{P}(n|n-1)$ corresponding to the channel estimation errors alone. It is seen that the UKF predicted covariance is significantly smaller than the L_2 channel error at lower SNRs. This is conjectured to be due to both the non-Gaussian statistics of the received signal which is amplified at lower SNR, as well as the effect of decision errors. At higher SNR, it is seen that the L_2 error norm approaches the trace covariance.

IV. Implementation Constraints and Homodyne Offset Estimator

The UKF-based algorithm is a state-of-the art nonlinear filtering solution to the cooperative MIMO channel estimation problem. However, it was determined that Kalman filter-based channel estimators were too complex for implementation in the current testbed [14]. This testbed employs the Xilinx Virtex-4SX FPGA for signal processing and currently implements an Alamouti 2x1 OSTBC at 500 kbps and a 1.3 GHz carrier frequency. Due to the FPGA constraints, a simplified homodyne frequency-offset estimator with LMS channel tracker was targeted to the Virtex device as described in [14]. Here, we show that the homodyne method is a systematic approximation to the ML joint delay/offset/channel estimator. The performance of the homodyne estimator is compared to the quasi-ML correlation and GSIC algorithms in [8].

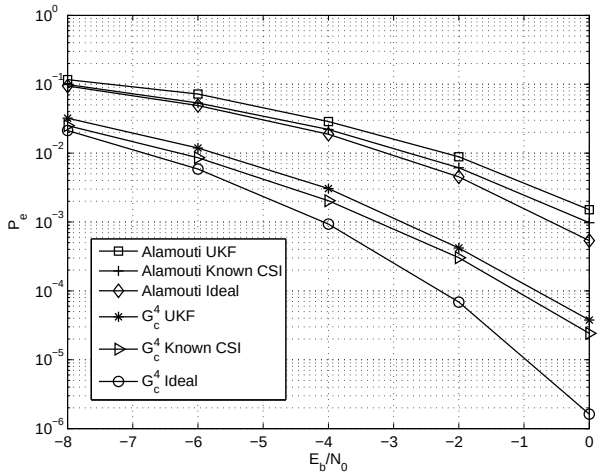

Fig. 2. BERs for UKF, perfect CSI and ideal orthogonal pulses.

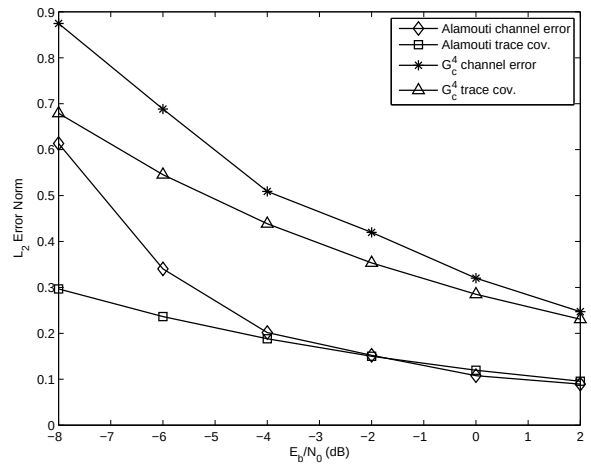

Fig. 3. Channel error comparison with UKF predicted covariance.

The homodyne method is introduced by considering a single sensor/single collector element received signal model. Set $N_s = M_c = 1$, with delay $\tau = 0$. Assume raised-cosine signaling with resulting zero intersymbol interference, and $T_s = T$ as the minimum Nyquist sampling interval. Then eq. (1) for the received signal matrix reduces to the sequence

$$r(n) = hs(n)e^{i\delta\omega nT_s} + n(n), \tag{19}$$

where $h \in \mathbb{C}$ is the scalar channel gain, and $s(n)$ is a training sequence. Consider the variables $u(n) = r(n)r^*(n+1)$. Then

$$u(n) = |h|^2 s(n)s^*(n+1)e^{-i\delta\omega T_s} + v(n), \tag{20}$$

where $v(n)$ depends on both the thermal noise $n(n)$ and transmitted signal. The following statistic is computed

$$\begin{aligned} g(\delta\omega) &= \sum_n s(n)^* s(n+1)u(n) \\ &\approx |h|^2 \left(\sum_n |s(n)|^2 |s(n+1)|^2 \right) e^{-i\delta\omega T_s} + \nu \end{aligned}. \tag{21}$$

An estimate of the frequency offset $\delta\omega$ is then just $\hat{\delta}\omega = -\text{arg} g(\delta\omega)/T_s$.

We next derive a homodyne algorithm for multiple sensors and collector elements for a quasi-static channel that jointly estimates the delays and channels. A TDMA transmission format is assumed during training, in which only sensor k transmits in each frame. First rewrite the received matrix (1) over an N_c symbol long training packet as

$$\begin{aligned} \mathbf{R} &= \sum_{q=0}^{N_c-1} s_k(q)(\mathsf{p}_q(\tau_k) \circ \mathbf{w}(\delta\omega_k))\mathbf{h}_k^T + \mathbf{N} \\ &= (\mathsf{s}_k(\tau_k) \circ \mathbf{w}(\delta\omega_k))\mathbf{h}_k^T + \mathbf{N}. \end{aligned} \tag{22}$$

In (22), the pulse function with zero frequency offset is defined by $\mathsf{p}_q(\tau_k) = \mathbf{p}_q(\tau_k, 0)$ in (2). The training sequence with zero frequency offset is $\mathsf{s}_k(\tau_k) = \sum_{q=0}^{N_c-1} s_k(q)\mathsf{p}_q(\tau_k)$, and the frequency vector $\mathbf{w}(\delta\omega)$ is

$$\mathbf{w}(\delta\omega_k) = \left[e^{i\delta\omega_k (N_c N_d - 1)T_s}, \ldots, e^{i\delta\omega_k T_s}, 1 \right]^T. \tag{23}$$

The joint ML estimate is

$$\hat{\tau}_k, \hat{\mathbf{h}}_k, \hat{\delta}\omega_k = \arg \min_{\tau_k, \mathbf{h}_k, \delta\omega_k} ||\mathbf{R}(n) - (\mathsf{s}_k(\tau_k) \circ \mathbf{w}(\delta\omega_k))\mathbf{h}_k^T||_F^2. \tag{24}$$

The channel estimate $\hat{\mathbf{h}}_k$ is first computed as

$$\hat{\mathbf{h}}_k = \frac{1}{||(\mathsf{s}_k(\tau_k)||^2} \mathbf{R}(n)^T (\mathsf{s}_k(\tau_k) \circ \mathbf{w}(\delta\omega_k))^*, \tag{25}$$

and substitution into (24) yields the delay/frequency estimates

$$\hat{\tau}_k, \hat{\delta}\omega_k = \arg \max_{\tau_k, \delta\omega_k} \frac{(\mathsf{s}_k(\tau_k) \circ \mathbf{w}(\delta\omega_k))^H \mathbf{R}(n)\mathbf{R}(n)^H (\mathsf{s}_k(\tau_k) \circ \mathbf{w}(\delta\omega_k))}{||(\mathsf{s}_k(\tau_k)||^2}. \tag{26}$$

To develop the Homodyne approximation, rewrite the maximization over $\delta\omega$ for fixed τ_k in (26) as

$$\hat{\delta}\omega_k = \arg \max_{\delta\omega_k} \sum_{l=0}^{N_c N_d - 1} \sum_{l'=0}^{N_c N_d - 1} e^{i\delta\omega_k (l'-l)T_s} \mathbf{A}(\tau_k)_{l,l'}. \tag{27}$$

where the matrix $\mathbf{A}(\tau_k)$ is defined by

$$\mathbf{A}(\tau_k) = \mathsf{s}_k(\tau_k)^H \circ \mathbf{R}(n)\mathbf{R}(n)^H \circ \mathsf{s}_k(\tau_k). \tag{28}$$

Note that with an abuse of notation, $\mathbf{R}(n)^H \circ \mathsf{s}_k$ corresponds to the Hadamard product of each row of $\mathbf{R}(n)^H$ with s_k. Changing variables yields

$$\hat{\delta}\omega_k = \arg \max_{\delta\omega_k} \sum_{\mu=-(N_c N_d - 1)}^{N_c N_d - 1} e^{i\delta\omega_k \mu T_s} \sum_{l=l_1(\mu)}^{l_2(\mu)} \mathbf{A}(\tau_k)_{l,l+\mu}, \tag{29}$$

where $l_1(\mu) = \max(0, -\mu)$ and $l_2(\mu) = \min(N_c N_d - 1, N_c N_d - 1 - \mu)$.

Define the cross-correlation coefficient

$$c(\tau_k, \mu) = \sum_{l=l_1(\mu)}^{l_2(\mu)} \mathbf{A}(\tau_k)_{l,l+\mu} \tag{30}$$

We now approximate $c(\tau_k, \mu) = 0$ for $\mu \neq \pm 1$. Note that $c(\tau_k, -\mu) = c(\tau_k, \mu)^*$, since matrix $\mathbf{A}(\tau_k)$ in (28) is Hermitian symmetric. Then an approximate frequency estimate for given τ_k is obtained by only using the terms $\mu = \pm 1$ in (29).

$$\begin{aligned} \hat{\delta}\omega_k &= \arg \max_{\delta\omega_k} \sum_{\mu=\pm 1} e^{i\delta\omega_k \mu T_s} c(\tau_k, \mu) \\ &= \arg \max_{\delta\omega_k} 2|c(\tau_k, 1)| \cos\left(\delta\omega_k T_s + \text{arg} c(\tau_k, 1)\right), \end{aligned} \tag{31}$$

which yields

$$\hat{\delta}\omega_k = -\text{ arg }(c(\tau_k, 1))/T_s. \tag{32}$$

The overall homodyne-based channel/delay/offset estimation algorithm is given in Table II.

It is next shown that the homodyne estimator (31) corresponds to (21) for $N_s = M_c = 1$ and $T_s = T$ for zero delay. In this case, the received vector is $\mathbf{r} = \mathsf{s}_k \circ \mathbf{w}(\delta\omega)h_k$, and the correlation coefficient becomes (assuming zero noise)

$$\begin{aligned} &c(\tau, 1) = \\ &\sum_{l=0}^{N_c N_d - 2} (\mathsf{s}^* \circ (\mathsf{s} \circ \mathbf{w}(\delta\omega))h)_l ((\mathsf{s} \circ \mathbf{w}(\delta\omega))^* h^* \circ \mathsf{s})_{l+1} \\ &= |h|^2 \sum_{l=0}^{N_c N_d - 2} (|(\mathsf{s})_l|^2)(\mathbf{w}(\delta\omega))_l (\mathbf{w}(\delta\omega)^*)_{l+1} (|(\mathsf{s})_{l+1}|^2) \\ &= e^{-i\delta\omega T_s} |h|^2 \sum_{l=0}^{N_c N_d - 2} (|(\mathsf{s})_l|^2)(|(\mathsf{s})_{l+1}|^2). \end{aligned}$$

Hence the coefficient is maximized when $\text{arg}(c(\tau_k, 1)) = -\delta\omega_k T_s$, and $\hat{\delta}\omega_k = -\text{ arg }(c(\tau_k, 1))/T_s$ yields the true frequency offset.

The algorithm in (31) was simulated for a quasistatic channel, where each realization of $\mathbf{h}_k$ was generated as i.i.d. circular Gaussian (Rayleigh fading.) Frequency offsets were chosen uniformly in the range ± 10 KHz. The frequency offset estimation error is shown in Fig. 4 for the homodyne method in Table II and the GSIC/correlation approximate ML estimators in [8]. It is seen that the homodyne estimator performance is unacceptable until > 20 dB SNR. This is evidently due to the approximation $c(\tau_k, \mu) = 0$ for $\mu \neq \pm 1$, since without this simplification, the homodyne can be shown to be equivalent to the correlation method in [8].

For sensors/packets $k = n = 1, \ldots, N_s$

Receive packet $\mathbf{R}(n)$ from sensor $k = m$

For delay hypotheses $q = 1, 2, \ldots Q$

Trial delay is $\tau = d_q$

Compute Hadamard training sequence/received matrix product

$$\mathbf{A}(d_q) = \mathsf{s}_k(d_q)^H \circ \mathbf{R}(n)\mathbf{R}(n)^H \circ \mathsf{s}_k(d_q)$$

Compute homodyne correlation coefficient

$$c(d_q, 1) = \sum_{l=0}^{N_c N_d - 2} \mathbf{A}(d_q)_{l,l+1}$$

Compute offset estimate

$$\hat{\delta}\omega(d_q) = -\arg(c(d_q, 1))/T_s$$

Metric computation

$$\gamma(d_q) = \sum_{l=0}^{N_c N_d - 1} \sum_{l'=0}^{N_c N_d - 1} e^{i\hat{\delta}\omega_k(d_q)(l'-l)T_s} \mathbf{A}(d_q)_{l,l'}$$

Next delay hypothesis d_q

$\hat{\tau}_k = \arg\max_{d_q} \gamma(d_q)$

$\hat{\delta}\omega_k = \hat{\delta}\omega_k(d_q)$

Channel estimate for sensor k

$$\hat{\mathbf{h}}_k = \frac{1}{||\mathsf{s}_k(\hat{\tau}_k)||^2} \mathbf{R}(n)^T (\mathsf{s}_k(\hat{\tau}_k) \circ \mathbf{w}(\hat{\delta}\omega_k)^*$$

Next sensor/packet $k = m$

TABLE II

HOMODYNE ALGORITHM FOR CHANNEL/OFFSET ESTIMATION.

The channel estimation error (sine-squared error) is compared for the homodyne, GSIC and correlation algorithms in Fig. 5. At higher SNR, the homodyne actually outperforms GSIC and correlation, apparently since the former employs TDMA transmission eliminating inter-sensor interference. Note that GSIC and correlation do not require TDMA, whereas homodyne performance was found to be unacceptable when all sensors transmit simultaneously.

V. CONCLUSIONS

Two joint estimators for cooperative MIMO systems were presented. The UKF method is an advanced nonlinear filtering algorithm that suffers a $< .5$ dB performance loss compared with perfect channel state information. In contrast, the current testbed based on FPGA technology can only implement a simplified homodyne estimator. It was shown that the homodyne is a systematic approximation to the joint ML estimator for quasi-static channels. However, simulated performance shows unacceptable offset errors except at very high > 20 dB SNRs. Thus, more advanced FPGA and ASIC technology is clearly required to implement Kalman-filter based tracking algorithms for the cooperative MIMO channel.

ACKNOWLEDGMENT

This work was supported by the Air Force Office of Scientific Research under Contract No. FA9550-05-C-0179 and Toyon Research Corporation Subcontract No. SC-06-5477-1.

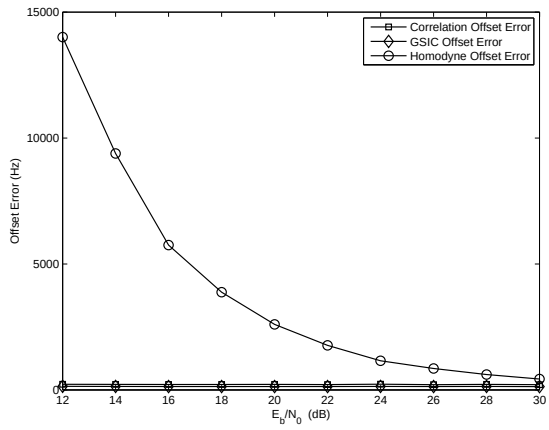

Fig. 4. Homodyne, GSIC and correlation offset estimation errors.

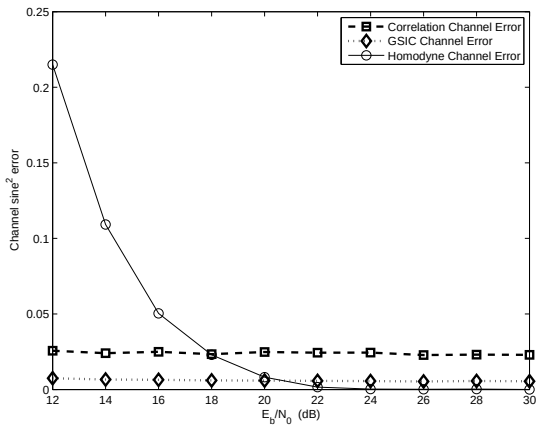

Fig. 5. Homodyne, GSIC and correlation sine-squared channel estimation errors.

REFERENCES

[1] J. N. Laneman and G. W. Wornell, "Distributed space-time-coded protocols for exploiting cooperative diversity in wireless networks," *IEEE Transactions on Information Theory*, vol. 49, pp. 2415–2425, Oct. 2003.

[2] S. Cui, A. Goldsmith, and A. Bahai, "Energy efficiency of MIMO and cooperative MIMO techniques in sensor networks," *IEEE Journal on Selected Areas in Communications*, vol. 22, pp. 1089–1098, Aug. 2004.

[3] S. J. Kim, R. E. Cagley, and R. A. Iltis, "Spectrally efficient communication for wireless sensor networks using a cooperative MIMO technique," *Wireless Networks*, 2006.

[4] V. Tarokh, H. Jafarkhani, and A. R. Calderbank, "Space-time block codes from orthogonal designs," *IEEE Transactions on Information Theory*, vol. 45, pp. 1456–1467, July 1999.

[5] O. Besson and P. Stoica, "On parameter estimation of MIMO flat-fading channels with frequency offsets," *IEEE Transactions on Signal Processing*, vol. 51, pp. 602–613, March 2003.

[6] S. Shahbazpanahi, A. Gershman, and J. Manton, "Closed-form blind MIMO channel estimation for orthogonal space-time block codes," *IEEE Transactions on Signal Processing*, vol. 53, pp. 4506–4517, 2005.

[7] S. Shahbazpanahi, A. Gershman, and G. Giannakis, "Joint blind channel and carrier frequency offset estimation in orthogonally space-time block coded MIMO systems," in *IEEE 6th Workshop on Signal Processing Adavances in Wireless Communications*, 2005, pp. 363–367.

[8] R. Iltis, S. Mirzaei, R. Kastner, R. Cagley, and B. Weals, "Carrier offset

and channel estimation for cooperative MIMO sensor networks," in *Proceedings of IEEE GLOBECOM*, San Francisco, CA, 2006.

[9] S. J. Julier and J. K. Uhlmann, "Unscented filtering and nonlinear estimation," *Proceedings of the IEEE*, vol. 92, pp. 401–422, March 2004.

[10] P. Garg, R. K. Mallik, and H. M. Gupta, "Exact error performance of square orthogonal space-time block coding with channel estimation," *IEEE Transactions on Communications*, vol. 54, pp. 430–437, Mar. 2006.

[11] M. Hata, "Empirical formula for propagation loss in land mobile radio services," *IEEE Transactions on Vehicular Technology*, vol. VT-29, pp. 317–325, Aug. 1980.

[12] B. Ristic, S. Arulampalam, and N. Gordon, *Beyond the Kalman Filter: Particle Filters for Tracking Applications*. Artech House, 2004.

[13] C. Komninakis, C. Fragouli, A. Sayed, and R. Wesel, "Multi-input multi-output fading channel tracking and equalization using Kalman estimation," *IEEE Transactions on Signal Processing*, vol. 50, pp. 1065–1076, May 2002.

[14] R. E. Cagley, B. T. Weals, and S. A. McNally, "Implementation of the Alamouti OSTBC to a distributed set of single-antenna wireless nodes," in *Proceedings of IEEE Wireless Communications and Networking Conference (WCNC)*, Hong Kong, 2007.